Scion Image software, the Windows version of National Institutes of Health Image (Scion Corp, Frederick, Md), were used in the other studies to measure the extent of GGOs in peripheral nonsmall cell lung cancer nodules objectively.[27,28] One study used the VR method, but measurements were performed quantitatively with a computer rather than visually.[27] That study concluded that future multicenter trials were needed to clarify the value of limited resection for clinical stage IA adenocarcinoma based on the extent of GGO determined with computer software. One limiting factor in that study that may affect interobserver measurement error is disagreement in the selection of the CT image that shows the nodule's largest cross-sectional area.[29] The other study used the area method,[28] and 1 limiting factor in that study that may affect interobserver measurement error is manual tracing of the areas of the tumor and solid component on the computer software.

Our study has several limitations. First, the scanning collimations and reconstruction intervals in the 5 medical institutions that actually provided thin-section CT images were not the same. The differences in scanning collimations and reconstruction intervals may have affected the evaluation of GGO and the solid component, thereby giving rise to interobserver measurement errors. Second, the lung-field window settings and mediastinal window settings may not have been optimized in the VR method. If the window width is set too wide or the window level is set too low in the Hounsfield units of the mediastinal window settings, the residual area of peripheral nonsmall cell lung cancer nodules becomes larger, resulting in a smaller VR percentage. If the VR method is to be used to select candidates for limited surgery, the most appropriate lung-field window and mediastinal window settings must be identified. Third, the visual measurements by the VR method cannot prevent intraobserver and interobserver measurement errors. One study found that tumor size was measured more accurately and consistently by readers who used an automated autocontour technique than by readers who used hand-held or electronic calipers.[26] Automated computer techniques need to be developed to reduce intraobserver and interobserver measurement errors.[30]

In conclusion, the VR method has the greatest ability to predict 5-year relapse-free survival in patients with peripheral nonsmall cell lung cancer. As a result of this finding, a prospective multicenter study of the VR method using automated computer techniques is warranted.

ACKNOWLEDGMENTS

The authors thank Junji Shiraishi, PhD, and Charles E. Metz, PhD, for providing the LABMRMC 1.0B3 software and assisting with the ROC curve analyses. The authors also thank Mrs Yoshie Iga for assistance in preparing the manuscript.

REFERENCES

1. Jang HJ, Lee KS, Kwon OJ, et al. Bronchioloalveolar carcinoma: focal area of ground-glass attenuation at thin-section CT as an early sign. *Radiology*. 1996;199:485–488.
2. Kuriyama K, Seto M, Kasugai T, et al. Ground-glass opacity on thin-section CT: value in differentiating subtypes of adenocarcinoma of the lung. *AJR Am J Roentgenol*. 1999;173:465–469.
3. Nakajima R, Yokose T, Kakinuma R, et al. Localized pure ground-glass opacity on high-resolution CT: histologic characteristics. *J Comput Assist Tomogr*. 2002;26:323–329.
4. Nakata H, Saeki H, Takata I, et al. Focal ground-glass opacity detected by low-dose helical CT. *Chest*. 2002;121:1464–1467.
5. Kodama K, Higashiyama M, Yokouchi H, et al. Natural history of pure ground-glass opacity after long-term follow-up of more than 2 years. *Ann Thorac Surg*. 2002;73:386–393.
6. Henschke CI, Yankelevitz DF, Mirtcheva R, et al. CT screening for lung cancer: frequency and significance of part-solid and nonsolid nodules. *AJR Am J Roentgenol*. 2002;178:1053–1057.
7. Aoki T, Tomoda Y, Watanabe H, et al. Peripheral lung adenocarcinoma: correlation of thin-section CT findings with histologic prognostic factors and survival. *Radiology*. 2001;220:803–809.
8. Nakata M, Sawada S, Saeki H, et al. Prospective study of thoracoscopic limited resection for ground-glass opacity selected by computed tomography. *Ann Thorac Surg*. 2003;75:1601–1606.
9. Kakinuma R, Ohmatsu H, Kaneko M, et al. Progression of focal pure ground-glass opacity detected by low-dose helical computed tomography screening for lung cancer. *J Comput Assist Tomogr*. 2004;28:17–23.
10. Li F, Sone S, Abe H, et al. Malignant versus benign nodules at CT screening for lung cancer: comparison of thin-section CT findings. *Radiology*. 2004;233:793–798.
11. Kodama K, Higashiyama M, Yokouchi H, et al. Prognostic value of ground-glass opacity found in small lung adenocarcinoma on high-resolution CT scanning. *Lung Cancer*. 2001;33:17–25.
12. Kim EA, Johkoh T, Lee KS, et al. Quantification of ground-glass opacity on high-resolution CT of small peripheral adenocarcinoma of the lung: pathologic and prognostic implications. *AJR Am J Roentgenol*. 2001; 177:1417–1422.
13. Takashima S, Maruyama Y, Hasegawa M, et al. Prognostic significance of high-resolution CT findngs in small peripheral adenocarcinoma of the lung: a retrospective study on 64 patients. *Lung Cancer*. 2002;36: 289–295.
14. Kondo T, Yamada K, Noda K, et al. Radiologic-prognostic correlation in patients with small pulmonary adenocarcinomas. *Lung Cancer*. 2002; 36:49–57.
15. Austin JM, Muller NL, Friedman PJ, et al. Glossary of terms for CT of the lung: recommendations of the Nomenclature Committee of the Fleischner Society. *Radiology*. 1996;200:327–331.
16. Matsuguma H, Yokoi K, Anraku M, et al. Proportion of ground-glass opacity on high-resolution computed tomography in clinical T1 N0 M0 adenocarcinoma of the lung: a predictor of lymph node metastasis. *J Thorac Cardiovasc Surg*. 2002;124:278–284.
17. Suzuki K, Asamura H, Kusumoto M, et al. "Early" peripheral lung cancer: prognostic significance of ground glass opacity on thin-section computed tomographic scan. *Ann Thorac Surg*. 2002;74:1635–1639.
18. Travis WD, Colby TV, Corrin B, et al, eds. *World Health Organization international histological classification of tumors. Histological typing of lung and pleural tumors*. 3rd ed. Berlin: Springer; 1999.
19. Noguchi M, Morikawa A, Kawasaki M, et al. Small adenocarcinoma of the lung. Histologic characteristics and prognosis. *Cancer*. 1995;75: 2844–2852.
20. Ohde Y, Nagai K, Yoshida J, et al. The proportion of consolidation to ground-glass opacity on high resolution CT is a good predictor for distinguishing the population of non-invasive peripheral adenocarcinoma. *Lung Cancer*. 2003;42:303–310.
21. Takamochi K, Nagai K, Yoshida J, et al. Pathologic N0 status in pulmonary adenocarcinoma is predictable by combining serum carcinoembryonic antigen level and computed tomographic findings. *J Thorac Cardiovasc Surg*. 2001;122:325–330.
22. Takamochi K, Yoshida J, Nishimura M, et al. Prognosis and histologic features of small pulmonary adenocarcinoma based on serum carcinoembryonic antigen level and computed tomographic findings. *Eur J Cardiothorac Surg*. 2004;25:877–883.
23. Shimizu K, Yamada K, Saito H, et al. Surgically curable peripheral lung carcinoma: correlation of thin-section CT findings with histologic prognostic factors and survival. *Chest*. 2005;127:871–878.
24. Okada M, Nishio W, Sakamoto T, et al. Discrepancy of computed tomographic image between lung and mediastinal windows as a

prognostic implication in small lung adenocarcinoma. *Ann Thorac Surg*. 2003;76:1828–1832.
25. Okada M, Nishio W, Sakamoto T, et al. Correlation between computed tomographic findings, bronchioloalveolar carcinoma component, and biologic behavior of small-sized lung adenocarcinomas. *J Thorac Cardiovasc Surg*. 2004;127:857–861.
26. Schwartz LH, Ginsberg MS, DeCorato D, et al. Evaluation of tumor measurements in oncology: use of film-based and electronic techniques. *J Clin Oncol*. 2000;18:2179–2184.
27. Matsugumа H, Nakahara R, Anraku M, et al. Objective definition and measurement method of ground-glass opacity for planning limited resection in patients with clinical stage IA adenocarcinoma of the lung. *Eur J Cardiothorac Surg*. 2004;25:1102–1106.
28. Nakata M, Sawada S, Yamashita M, et al. Objective radiologic analysis of ground-glass opacity aimed at curative limited resection for small peripheral non-small cell lung cancer. *J Thorac Cardiovasc Surg*. 2005; 129:1226–1231.
29. Revel MP, Bissery A, Bienvenu M, et al. Are two-dimensional CT measurements of small noncalcified pulmonary nodules reliable? *Radiology*. 2004;231:453–458.
30. Bellon E, Feron M, Maes F, et al. Evaluation of manual vs semi-automated delineation of liver lesions on CT images. *Eur Radiol*. 1997;7:432–438.

NOTICE OF DUPLICATE PUBLICATION

Upon receiving correspondence from a concerned reader, Editors of the *Journal of Computer Assisted Tomography, Radiology, Investigative Radiology*, and *Journal of Invasive Cardiology* recently reviewed a number of articles submitted to our respective journals authored by Dr. Bin Lu and colleagues during the period 2000–2002.

Five of these articles appeared in *JCAT*, and our internal analysis revealed no evidence of plagiarism, data falsification, or any problems with these particular manuscripts.

However, a later paper published by Lu et al[1] in a Chinese language journal clearly contains large segments of identical text, tables, and/or duplicated figures without credit to the original *JCAT* source.[2] Some apparent duplication of data from another *JCAT* paper[3] also appears in a 2002 article from the *Journal of Invasive Cardiology*[4] and a 2004 article in the *Chinese Journal of Radiology*.[5] It is my understanding that unexplained data inconsistencies may be present in certain of these derivative non-*JCAT* articles, but the data originally published in *JCAT* appears to be sound.

Dr. Lu has been appraised of these findings and is apologetic about the appearance of *JCAT* text and data appearing in other later publications without proper citation or credit.

Allen D. Elster, MD, FACR
Editor-in-Chief

REFERENCES

1. Lu B, Dai R, Jing B, et al. Evaluation of coronary artery bypass graft patency using three-dimensional reconstruction and flow study of electron beam tomography. *Chin Med J*. 2001;114(5):466–472.
2. Lu B, Dai R-P, Jing B-L, et al. Evaluation of coronary artery bypass graft patency using three-dimensional reconstruction and flow study on electron beam tomography. *J Comput Assist Tomogr*. 2000;24(5):663–670.
3. Lu B, Zhuang N, Mao S-S, et al. Image quality of three-dimensional electron beam coronary angiography. *J Comput Assist Tomogr*. 2002;26(2):202–209.
4. Lu B, Dai R-P, Zhuang N, et al. Noninvasive assessment of coronary artery bypass graft patency and flow characteristics by electron-beam tomography. *J Invas Cardiol*. 2002;14:19–24.
5. Lu B, Zhuang N, Dai R-P, et al. Evaluation of coronary calcium scoring versus electron-beam CT angiography for segmental analysis of coronary artery stenosis. *Chin J Radiol*. 2004;38(12):1305–1310.

論　文

肺がんCT検診の業務支援システム

石垣　陸太[†a)]　花井　耕造[††]　鈴木　雅裕[†††]　河田　佳樹[††††]
仁木　登[††††]　江口　研二[†††††]　柿沼龍太郎[†††]　森山　紀之[†††]

An Operating Support System for Lung Cancer CT Screening

Rikuta ISHIGAKI[†a)], Kouzou HANAI[††], Masahiro SUZUKI[†††], Yoshiki KAWATA[††††], Noboru NIKI[††††], Kenji EGUCHI[†††††], Ryutaro KAKINUMA[†††], and Noriyuki MORIYAMA[†††]

あらまし　現在，日本において肺がんの総死亡数は男性で1位，女性で3位である．この死亡者数は毎年増加傾向にあり，早期発見及び早期治療が求められている．このために肺がんCT検診が始まっている．この検診業務は事務部門，放射線部門，診断部門の3部門に大別され，これらは紙ベースの運用や既存の電子カルテシステムと紙ベースを併用した運用で実施されている．本論文では，検診業務を効率良く運用する肺がんCT検診の業務支援システムについて述べる．このシステムは(1)業務工程の分析，(2)業務情報の電子化，(3)業務情報の可視化について研究開発している．本システムをCT検診施設で使用して各部門の業務処理時間，ユーザアンケート調査によって有効性を示す．

キーワード　肺がんCT検診，データベース，業務支援システム

1. まえがき

医療制度改革の一環として一次予防に重点をおいた健康増進法[1]の施行があり，国民の健康維持の推進を図っている．がん対策として，がん検診指針が示され，受診率の向上と死亡率減少効果が期待される検診を推奨している[2],[3]．臓器別にがん研究が多分野で進められている．

肺がんにおいては，早期発見を目的にX線CTを利用して肺がん死の低減を図ろうとする肺がんCT検診（以下，CT検診）が始まっている．

CT検診は1996年のKanekoら[4]，1998年のSoneら[5]，1999年にはHenschkeら[6]によるCT検診の有効性が報告されている．

がん検診の方法論は科学的に検証することが求められ[7]，CT検診においても様々な研究が盛んに行われている[8]～[10]．CT検診の実施形態は，自治体検診，職域検診，人間ドックなどがあり[11]，実施機関については，検診専門機関，一般医療機関，高度専門医療機関と様々な特徴ある機関で実施されている[12]～[14]．この検診業務を担当する部門は，事務部門，放射線部門及び診断部門である．この3部門間で受診者の情報が流通する構図である．この中で業務効率と正確性の向上を図ることは重要である．現行の検診業務フローは，紙ベース（情報媒体は紙を使用）を用いた運用や既存の電子カルテシステムと紙ベースを併用した運用であるため検査遅延が発生して非効率的な状況にある．住民の健康診断に自治体などの予算を使用してCT検診受診を勧奨しており，受診者数の増加を考慮すると早急に効率的な運用が必要である[15],[16]．

医療情報システムは，受診者の病歴や健康状態を記

† 京都医療科学大学，南丹市
Kyoto College of Medical Science, 1-3 Imakita, Oyama-Higashi, Sonobe-cho, Nantan-shi, 622-0041 Japan
†† 国立がんセンター東病院，柏市
National Cancer Center Hospital East, 6-5-1 Kashiwanoha, Kashiwa-shi, 277-8577 Japan
††† 国立がんセンターがん予防・検診研究センター，東京都
Research Center for Cancer Screening and Prevention, National Cancer Center, 5-1-1 Tsukiji, Chuo-ku, Tokyo, 103-0045 Japan
†††† 徳島大学大学院ソシオテクノサイエンス研究部，徳島市
Institute of Technology and Science, The University of Tokushima, 2-1 Minamijosanjima-cho, Tokushima-shi, 770-8506 Japan
††††† 帝京大学医学部，東京都
Department of Medicine, University of Teikyo, 2-11-1 Kaga, Itabashi-ku, Tokyo, 173-8605 Japan
a) E-mail: rikuta@kyoto-msc.jp

録，検索，表示する電子カルテシステム [17], [18]，及び医師からの各検査の指示や治療指示を迅速に表示・実施記録の保管を目的にするオーダリングシステム [19] がある．また，薬剤管理等を行う部門システムや医事会計システムなどもある．これらのシステムが相互に連動して臨床現場で利用されている．

検診現場では紙ベースの運用や受診施設の規模に応じた電子カルテシステムと紙ベースを併用した運用がなされている [20]．しかし，電子カルテシステムは受診者管理に重点を置いたシステムであり，検診現場では CT 検診，乳がん検診，脳ドックなど臓器ごとに業務工程が異なっており，業務効率を更に向上させるためには臓器ごとに必要とする業務情報を的確に提供する業務支援システムが求められる．

本論文では，(1) 業務工程の分析，(2) 業務情報の電子化，(3) 業務情報の可視化について研究してシステム化する．開発したシステムを検診現場で運用して各部門での業務処理時間，ユーザアンケート調査によって有効性を示す．

2. では CT 検診の業務支援システムの課題，3. では CT 検診業務支援システムの構成について，4. では CT 検診業務支援システムの実現と評価について述べる．

2. CT 検診の業務支援システムの課題

2.1 CT 検診業務

CT 検診業務は，図 1 に示す事務部門，放射線部門，診断部門の三つの部門で構成されている．事務部門は，予約管理，カルテ作成，判定結果郵送処理の業務を実施する．放射線部門は，問診票の記入依頼，CT 検査業務を実施する．診断部門は，問診票参照，診断業務を実施する．図 2 は検診業務工程を新規受診者，経年受診者，要精査者の受診者別に分析した業務フローを示す．これは紙ベースの運用や受診施設の規模に応じた電子カルテシステムと紙ベースを併用した運用がなされている．

2.2 CT 検診業務の課題

CT 検診の業務は，受診者数が 1 日当り 100 人程度を対象としているため，大量の画像情報やテキスト情報が発生する．各部門の職員は図 2 の業務工程を正確な情報で迅速にすることが求められる．業務処理を向上させるために各部門での課題は以下のとおりである．

(1) 事務部門：紙ベース運用では受診調査（フィルム探し，カルテ探し），受診者 ID（氏名，年齢，性別，生年月日）の登録，判定結果送付作業が非効率である．電子カルテシステムでは受診調査，受診者 ID の登録などは実現しているが，判定結果送付先の情報，業務内容の進捗情報の表示などは実現されていない．

(2) 放射線部門：紙ベース運用では問診票のカルテとじ，受診者別に応じた以前の判定結果と病変位置の確認が非効率である．また，電子カルテシステムでは問診票回答の入力，以前の判定結果や病変位置の画像について実現されているが，受診者別の病変画像（病変の中心部が撮影されている画像）と受診歴を連動させて効率良く表示されているものはない．

(3) 診断部門：紙ベース運用では問診票，受診歴，読影レポート作成が非効率である．電子カルテシステムでは問診票の設問と回答文言が分かりやすく表示されるものはない．また，1 画面で問診票，受診歴，病変詳細情報を集約して扱えるものがない．

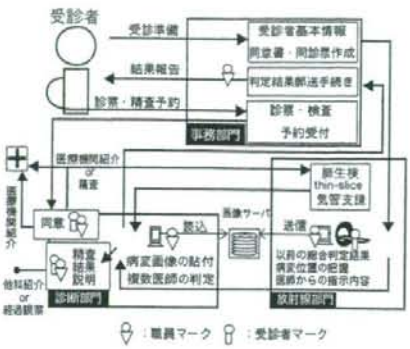

図 1 CT 検診の業務
Fig. 1 Work of CT screening for lung cancer.

図 2 受診者別の業務フロー
Fig. 2 Workflow of each subjects.

2.3 CT 検診業務の課題の対応

各部門での課題の対応は以下のとおりである．

（1） 事務部門：受診調査，受診者 ID の登録に加えて判定結果送付先の情報，業務内容の進捗情報を電子化して可視化する．

（2） 放射線部門：問診票回答の入力，受診者別に応じた以前の判定結果と病変位置確認に加えて実施済み入力，フィルムラベル作成，受診者別の病変画像と受診歴を連動させて表示する機能を電子化して可視化する．

（3） 診断部門：1 画面に問診票，受診歴，病変詳細情報を集約し，これを電子化して可視化する

図 3 に各部門の業務フローの中で電子化して可視化する部分を黒色背景にして示す．

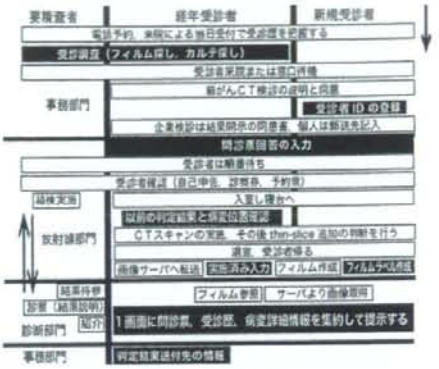

図 3 業務情報の電子化・可視化部分
Fig. 3 Electronics data visualization parts.

3. CT 検診業務支援システムの構成

3.1 業務支援システムの構成

2.3 で述べた課題に対応する業務支援システムについて述べる．CT 検診業務支援システムの構成を図 4 に示す．システムの核となる受診者情報は（1）受診者 ID，（2）受診者市町村コード・Zip コード（郵便番号），（3）業務内容の進捗情報，（4）業務管理情報（検査使用物品の情報・業務報告・照射録），（5）受診者の予約情報，（6）受診歴，（7）判定結果情報，（8）病変詳細情報，（9）病変画像情報，（10）問診情報からなる．この中で（3）業務内容の進捗情報，（4）業務管理情報，（8）病変詳細情報，（9）病変画像情報は CT 検診現場に特有な四つの情報である．これらを黒色背景で示す．

受診者情報はカード型データモデル [21] で表現されてデータベース化され，受診者全情報，全市町村コード・Zip コード，全病変画像の三つのデータベースとリレーションしている．受診者全情報は受診者 ID で，全市町村コード・Zip コードは受診者市町村コード・Zip コードの郵便番号で連結される．病変画像情報は全病変画像と連結して直接貼付する．受診歴は受診者情報の重複登録を利用して自己リレーションする．

このデータベースを事務部門支援画面，放射線部門支援画面，診断部門支援画面より各部門の担当者が入力，検索，参照して利用する．各部門より入力，検索及び参照するための効率的な操作画面を作成する．

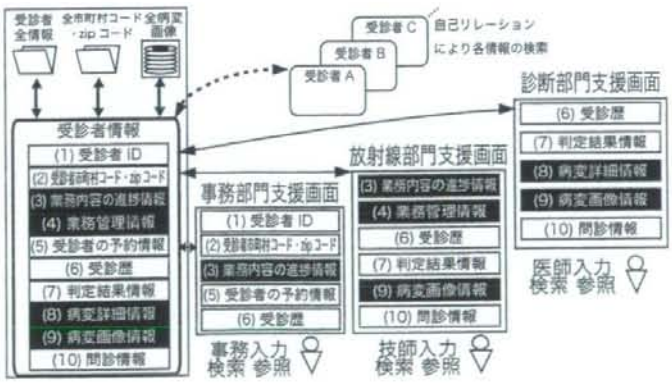

図 4 CT 検診業務支援システムの構成
Fig. 4 Relationship of information structure.

3.2 各部門の業務支援情報の可視化

事務部門での受診者情報として（1）受診者 ID，（2）受診者市町村コード・Zip コード，（3）業務内容の進捗情報，（5）受診者の予約情報，（6）受診歴の五つの情報を取り扱う．放射線部門の（4）業務管理情報，（10）問診情報や診断部門の（7）判定結果情報が決定されると（3）業務内容の進捗情報へ反映されるようにする．

放射線部門での受診者情報として（3）業務内容の進捗情報，（4）業務管理情報，（6）受診歴，（7）判定結果情報，（9）病変画像情報，（10）問診情報を取り扱う．技師は診断部門のために（10）問診情報を電子化し，（9）病変画像情報より病変位置確認ができるようにする．

診断部門での受診者情報として（6）受診歴，（7）判定結果情報，（8）病変詳細情報，（9）病変画像情報，（10）問診情報を取り扱う．（7）判定結果情報，（9）病変画像情報，（10）問診情報は次回受診時に（6）受診歴として残す情報である．

各部門で取り扱う必要な情報を集約して入力，検索，参照できる画面設計にする．

4. CT 検診業務支援システムの実現と評価

4.1 業務支援システム

本システムは CT 検診業務に特化したものであり，関係する部門も 3 部門と少ないため構築は比較的容易である．この業務支援システムの構築を図 5 に示す．ホストを立て 4 台のコンピュータで相互運用している．表 1 にハードウェアの構成を示す．また本システムの汎用性を向上させるためにファイル共有型からクライアントサーバ環境型まで幅広く対応できる FileMaker を使用した[22]．これは各検診機関への領布後カスタマイズやこれまでの蓄積データを移行する場合も比較的容易にできる．

4.2 事務部門での業務支援画面

図 6 に事務部門の業務支援画面を示す．図 6 に示した番号は **3.1** で述べた受診者情報の（1）から（10）の番号に対応する．この画面上部は（3）業務内容の進捗情報，（7）判定結果情報を表示し，画面中部は（1）受診者 ID，（2）受診者市町村コード・Zip コード，（4）業務管理情報，（9）病変画像情報（拡大病変画像ボタン）を表示している．画面下部は（5）受診者の予約情報，（6）受診歴を表示する．（6）受診歴では 3 名の医師の判定結果を示している．画面最下部は画面切換ボタンや印刷機能ボタンである．これらのボタンは各部門において利用制限機能を設けている．事務部門で（1）受診者 ID，（2）受診者市町村コード・Zip コード，（5）受診者の予約情報を入力し，（3）業務内容の進捗情報，（6）受診歴の情報を参照して業務を実施する．これらの利用状況に関する履歴を残している．

4.3 放射線部門での業務支援画面

放射線部門の業務支援画面は図 6，図 7，図 8 であ

表 1 ハードウェアの構成
Table 1 Hardware configuration.

Hardware	OS	CPU memory・HDD 容量
Host machine	Windows XP	Pen.4 3.0 GHz 2 GB・120 GB
Client machine1	Windows XP	Celeron.M 1.3 GHz 256 MB・40 GB
Client machine2	Windows XP	Pen.4 3.0 GHz 2 GB・120 GB
Client machine3	Mac OSX	Core2Duo 2.16 GHz, 2 GB・160 GB

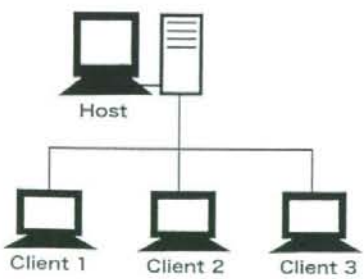

図 5 システム構成
Fig. 5 System configuration.

図 6 事務部門の業務支援画面
Fig. 6 Supported screen in the information office.

図 7 放射線部門の業務支援画面（問診画面）
Fig. 7 Supported screen in the department of radiology (interview screens).

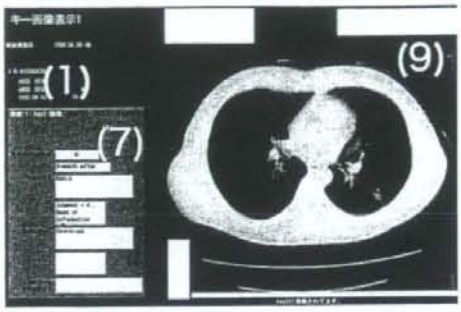

図 8 放射線部門の業務支援画面（病変画像と判定結果の画面）
Fig. 8 Supported screen in the department of radiology (screen of a pathological change picture and a judgment result).

る．図 7，図 8 に示した番号は **3.1** で述べた受診者情報の（1）から（10）の番号に対応する．図 6 の（1）受診者 ID，（3）業務内容の進捗情報，（6）受診歴を参照し，（4）業務管理情報を入力する．図 6 の画面切換ボタンにより図 7 の問診画面を選択し，（10）問診情報を入力する．図 6 の（6）受診歴と（9）病変画像情報によって受診者別の病変画像と受診歴を連動表示させている．（6）受診歴中にある KEY ボタンと（9）病変画像情報（拡大病変画像ボタン）によって図 8 に切り換わり，図 8 の右半分は（9）病変画像情報の表示，左半分は（1）受診者 ID，（7）判定結果情報の表示である．図 8 を参照して以前の判定結果と病変位置の確認を行う．

4.4 診断部門での業務支援画面

診断部門の業務支援画面を図 9 に示す．図 9 に示した

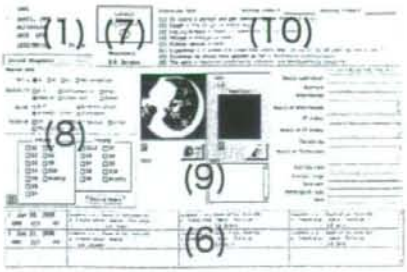

図 9 診断部門の業務支援画面
Fig. 9 Supported screen in the diagnosis section.

番号は **3.1** で述べた受診者情報の（1）から（10）の番号に対応する．この画面上部は（1）受診者 ID，（7）判定結果情報，（10）問診情報を表示している．（10）問診情報は容易に理解できるように回答文言が表示されている．画面中部は（8）病変詳細情報，（9）病変画像情報が表示されている．画面下部は（6）受診歴を表示している．診断部門で（8）病変詳細情報，（9）病変画像情報を入力する．1 画面で（6）受診歴，（8）病変詳細情報，（10）問診情報を集約して表示している．

4.5 業務支援システム導入前後の各部門での業務処理時間の比較評価

図 3 で示した業務処理時間を評価項目別に比較した結果を図 10 に示す．

導入前後の業務処理時間を比較評価するために 10 名の受診者を選択し，事務員 2 名，技師 2 名，医師 2 名で業務処理時間を評価した．導入前の検診業務の経験年数は，事務員 A が 6 か月，B が 4 か月であり，技師 2 名と医師 2 名については 6 か月である．導入後は，1 年 4 か月のときに業務処理時間を評価した．

事務部門の評価項目は，受診歴の把握までに要す時間（M1），受診者 ID の登録時間（M2），業務内容の進捗情報の把握と判定結果送付作業完了に要す時間（M3）の 3 項目である．放射線部門の評価項目は，問診票回答に要す時間（M4），以前の判定結果，病変画像情報より病変位置の確認に要す時間（M5），実施済み入力とフィルムラベル作成時間（M6）の 3 項目である．診断部門の評価項目は問診票・受診歴・病変画像情報参照後に読影開始までの時間（M7）の 1 項目である．全部門の評価項目は業務処理時間を合計した処理時間（M8）である．

事務部門の課題で対応した受診調査は（M1）で，受診者 ID の登録は（M2）で，判定結果送付先の情報

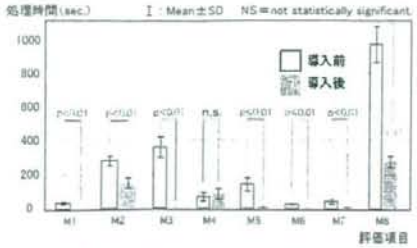

図 10 導入前後での効果を時間比較
Fig. 10 Time compares the effect in introduction order.

と業務内容の進捗情報は（M3）で評価している．放射線部門の課題で対応した問診票回答の入力は（M4）で，以前の判定結果と病変位置確認と受診者別の病変画像と受診歴を連動させる表示は（M5）で，実施済み入力，フィルムラベル作成は（M6）で評価している．診断部門で対応した 1 画面に問診票，受診歴，病変詳細情報を集約して表示することは（M7）で評価している．

また，CT 検診現場において特有の四つの情報（(3) 業務内容の進捗情報，(4) 業務管理情報，(8) 病変詳細情報，(9) 病変画像情報）と各評価項目との関連について述べる．(3) は（M3）に関与し，(4) は（M6）に関与し，(8) と (9) は（M7）に関与している．

導入前後の業務処理時間について評価項目別に平均時間，標準偏差を算出して評価項目別の業務処理時間を Paired-t 検定を用いて有意差検定を行った．

評価項目別の導入前後の業務処理時間の平均時間，最大時間，最小時間を表 2 に示す．全部門での平均業務処理時間の平均時間が 16.2 分から 4.6 分となり約 1/4 に短縮された．この平均業務処理時間は CT 検診現場で効率的に運用できる時間となった．また，M4 の問診票回答に要す時間以外は有意差（$p < 0.01$）を認め，統計学的に本システムの有効性が示された．導入前の M4 は受診者が問診票に記載し技師がカルテにとじる作業の時間であり，導入後の M4 は面談式で技師が問診項目について受診者へたずねて回答を入力するまでの時間である．M7 は 1 画面で (6) 受診歴，(8) 病変詳細情報，(10) 問診情報を集約して電子化することで医師らの読影開始までの時間を短縮できた．M3 では電子化することでカルテ探しや電話連絡の業務処理の平均時間が 6 分から 4.6 秒まで短縮した．M5 の業務処理の平均時間は 2.4 分から 13.2 秒まで短縮され，2 名の技師で分担していた過去のフィルム画像の病変確認作業を 1 名の技師で迅速に実現可能となった．

表 2 導入前後での計測時間の詳細
Table 2 Details of the measurement time in introduction order.

導入前 [s]			
評価項目	平均時間	最大時間	最小時間
M1	38.4	50.3	30.2
M2	285.7	330.6	247.3
M3	361.9	480.4	293.1
M4	72.0	117.2	30.5
M5	145.1	220.4	90.2
M6	26.9	40.1	19.2
M7	45.0	67.6	21.8
M8	975.1	1193.9	844.6

導入後 [s]			
評価項目	平均時間	最大時間	最小時間
M1	5.6	8.1	3.4
M2	150.6	191	100
M3	4.6	5.9	3.5
M4	86.5	125	44
M5	13.2	21.4	7.9
M6	5.7	7	4.5
M7	11.5	18.3	5.4
M8	277.6	343	225.7

4.6 アンケート調査

本システムの業務支援機能の有効性を評価するため稼動中の 1 施設における事務員 2 名，技師 2 名，医師 2 名に対して 2007 年 7 月にアンケートを実施した．それぞれの担当者に「満足」（5 点），「やや満足」（4 点），「普通」（3 点），「やや不満」（2 点），「不満」（1 点）の 5 段階評価方式で有効性を評価した．以下にアンケートの設問を示す．

（Q1）「他部門との情報共有に役立つ」効果はありますか？（3 部門共通）

（Q2）「直感的な操作」について効果はありますか？（3 部門共通）

（Q3）「事前に受診歴を迅速に参照できる」効果はありますか？（事務部門の業務支援画面）

（Q4）「進捗状況を把握する」効果はありますか？（事務部門の業務支援画面）

（Q5）「病変画像，病変位置の把握，判定結果表示，指示内容表示画面」の履歴情報について効果はありますか？（放射線部門の業務支援画面）

（Q6）「問診票入力は以前の紙と比較して」効果はありますか？（放射線部門の業務支援画面）

（Q7）「以前の判定結果，問診票，病変画像を参照し判定すること」について効果はありますか？（診断部門の業務支援画面）

表 3 アンケートの評価結果
Table 3 Result of questionnaire.

事務部門		放射線部門		診断部門	
問	評価点	問	評価点	問	評価点
Q1	4.5	Q1	4.0	Q1	3.5
Q2	4.0	Q2	4.5	Q2	4.5
Q3	5.0	Q5	5.0	Q7	5.0
Q4	5.0	Q6	5.0		

(Q8) 本システムは CT 検診業務に関してどのような効果がありましたか．また，システムの改善点があれば記述してください．(3 部門共通)

(Q1)，(Q2)，(Q8) は各部門共通の設問である．(Q3)，(Q4) は事務部門に対する設問である．(Q5)，(Q6) は放射線部門に対する設問，(Q7) は診断部門に対する設問である．

事務部門の課題で対応した受診調査は (Q3) で，判定結果送付先の情報と業務内容の進捗情報については (Q4) である．放射線部門の課題で対応した問診票回答の入力は (Q6) で，以前の判定結果と病変位置確認と受診者別の病変画像と受診歴を連動させる表示は (Q5) である．診断部門の課題で対応した 1 画面に問診票，受診歴，病変詳細情報を集約して表示することは (Q7) である．

また，CT 検診現場において特有の四つの情報 ((3) 業務内容の進捗情報，(4) 業務管理情報，(8) 病変詳細情報，(9) 病変画像情報) と各設問との関連について述べる．(3) は (Q1) と (Q4) に関与し，(4) は (Q1) に関与し，(8) と (9) は (Q5) と (Q7) に関与している．

アンケート結果を表 3 に示す．(Q1) は事務員及び技師ともに「やや満足」であった．医師は「普通」であった．(Q2) は事務員，技師，医師ともに「やや満足」であった．事務部門に関する (Q3)，(Q4) は「満足」と評価された．放射線部門に関する (Q5)，(Q6) は「満足」と評価された．診断部門に関する (Q7) は「満足」と評価された．本システムは総合的に高く評価された．

(Q8) に関しては，「導入前と比較して担当職員の情報共有ができて受診者に余裕をもって対応することができた」と意見があった．また，システムの改善点についての意見として，「コンピュータ支援診断システムが指摘した画像を保管できるようにしてほしい」，「医用画像ビューアとの連動と統計データの項目を追加してほしい」と意見があった．これらは今後の課題である．

5. むすび

CT 検診現場では紙ベースの運用や受診施設の規模に応じた電子カルテシステムと紙ベースを併用した運用がなされている．業務効率を更に向上させるための業務支援システムの開発が求められた．本論文では，(1) 業務工程の分析，(2) 業務情報の電子化，(3) 業務情報の可視化について研究してシステム化した．開発したシステムを CT 検診現場で運用して各部門での業務処理時間，ユーザアンケート調査によって有効性を示し，業務の負担を軽減し効率良く迅速に運用できることが示唆された．

本 CT 検診業務支援システムは，「低線量肺がん CT 検診の手引き」[7] の付録として無償提供され，現在 4 施設で運用している．

今後は，CT 検診現場からの問題点の改善や臓器別がんに対応できる検診業務支援システムへと開発を進める予定である．

謝辞 本研究を進めるにあたり，御協力頂きました独立行政法人国立病院機構神奈川病院の放射線科に感謝致します．また，本研究は平成 19 年度厚生労働省科学研究費補助金 (第三次対がん総合戦略研究事業) の研究項目「コンピュータ支援がん画像診断装置によるがん精度・効率向上に関する研究」より助成されたものである．

文献

[1] 厚生労働省，"健康増進法，" 平成 14 年 8 月 2 日法律第 103 号，2002.
[2] 厚生労働省，"がん予防重点教育及びがん検診の実施のための指針について，" 老健第 64 号，平成 10 年 3 月 31 日，1998.
[3] 厚生労働省，"がん予防重点教育及びがん検診の実施のための指針の一部改正について，" 老老発第 0427001 号，平成 16 年 4 月 27 日，2004.
[4] M. Kaneko, K. Eguchi, H. Ohmatsu, R. Kakinuma, T. Naruke, K. Suemasu, and N. Moriyama, "Peripheral lung cancer: screening and detection with low-dose spiral CT versus radiography," Radiology, vol.201, pp.798–802, 1996.
[5] S. Sone, S. Takashima, F. Li, Z. Yang, T. Honda, Y. Maruyama, M. Hasegawa, T. Yamada, K. Kubo, K. Hanamura, and K. Asakura, "Mass screening for lung cancer with mobile spiral computed tomography scanner," Lancet, vol.351, pp.1242–1245, 1998.
[6] C.I. Henschke, D.I. Mccauley, D.F. Yankelevits, D.P. Naidich, G. McGuinness, O.S. Miettinen, D.M. Libby, M.W. Pasmantier, J. Koizumi, N.K. Altorki,

and J.P. Smith, "Early lung cancer action project: Overall design and finding from baseline screening," Lancet, vol.354, pp.99–105, 1999.
[7] 江口研二, 他, "低線量 CT による肺癌検診の手引き," 低線量 CT による肺癌検診のあり方に関する合同委員会見解 2004, pp.1–3, 金原出版, 東京, 2004.
[8] N. Niki, Y. Kawata, M. Kubo, H. Ohmatsu, R. Kakinuma, M. Kaneko, M. Kusumoto, and N. Moriyama, "A CAD system for lung cancer based on 3D CT images," CARS, pp.701–705, 2002.
[9] Y. Kawata, N. Niki, H. Ohmatsu, M. Kusumoto, and R. Kakinuma, "A visual data-mining approach using 3-D thoracic CT images for classification between benign and malignant pulmonary nodules," Proc. SPIE Medical Imaging, pp.1375–1385, 2003.
[10] K. Hanai, T. Horiuchi, J. Sekiguchi, Y. Muramatsu, R. Kakinuma, N. Moriyama, R. Tuchiiya, and N. Niki, "Computer-simulation technique for low dose computed tomographic screening," J. Comput. Assist Tomogr., vol.30, no.6, pp.955–961, Nov./Dec. 2006.
[11] 中山富雄, 佐川元保, 遠藤千顕, 濱島ちさと, 斉藤 博, 祖父江友孝, "有効性評価に基づく肺がん検診ガイドラインの作成," 日本 CT 検診学会誌, vol.13, no.3, pp.225–230, 2006.
[12] 大松広伸, "「東京から肺がんをなくす会」の実施成績," 東京都予防医学協会年報, vol.36, pp.150–154, 2007.
[13] 石垣陸太, 長澤宏文, 佐藤 勝, 鯵坂幸宏, 花井耕造, 杉尾敏憲, "胸部 CT 検診のためのデータファイル構築について," 胸部 CT 検診, p.53, 2003.
[14] 中山富雄, 楠 洋子, 鈴木隆一郎, 有澤 淳, 黒田知純, 潤間隆宏, 長尾啓一, 滝口裕一, 栗山喬之, 松本 徹, "肺癌 CT 検診ネットワーク読影に関するデータベースシステムの構築," 日本肺癌学会誌, vol.41, no.5, p.475, 2001.
[15] 厚生労働省, "市町村事業における肺がん検診の見直しについて中間報告案," 平成 19 年 12 月, 2007.
[16] 厚生労働省, "平成 14 年労働者健康状況調査の概況," 平成 15 年 8 月, 2002.
[17] 里村洋一, "電子カルテの登場とその背景," 電子カルテが医療を変える, pp.7–35, 日経 BP 社, 1998.
[18] 藤原一央, "放射線治療部門での電子カルテ導入による効率化," 新医療, no.374, pp.63–66, 2006.
[19] 宇都由美子, 村永文学, 熊本一朗, "オーダリングシステムによる病院情報システムの構築," 医療情報学, vol.19, suppl, pp.10–13, 1999.
[20] 木村直男, 電子カルテ・医療情報システム部品集 2007, 株式会社インナービジョン, CD-ROM, 東京, 2006.
[21] 梅棹忠夫, 知的生産の技術, 岩波書店, 東京, 1980.
[22] 高岡幸生, ファイルメーカー Pro Web データベース講座, pp.320–323, オーム社, 東京, 2004.

（平成 20 年 3 月 7 日受付, 5 月 15 日再受付）

石垣 陸太 （正員）

1994 京都医療技術短大・放射線技術卒, 2007 京都医療科学大学助教. 現在, 徳島大学大学院博士後期課程在学中. 医療情報システムの研究に従事.

花井 耕造

1974 阪大・医療技術短大卒. 1980 東京理科大・理学部二部卒. 2007 徳島大学博士後期課程了. 工博（徳大）. 2008 より国立がんセンター東病院技師長.

鈴木 雅裕

2002 中央医療技術専門学校診療放射線学科卒. 2004 国立がんセンターがん予防・検診研究センター. 2007 国立がんセンター中央病院とがん予防・検診研究センター併用. 現在, 徳島大学大学院博士後期課程在学中.

河田 佳樹 （正員）

1995 徳島大学大学院博士後期課程了. 2004 同大・工・光応用工学科准教授. 博士（工学）, 医用イメージングに関する研究に従事.

仁木 登 （正員）

1977 徳島大学大学院工学研究科了. 1996 同大学工学部光応用工学科教授. X 線 CT イメージング, コンピュータ支援診断に関する研究に従事. 工博（京大）. 日本医用画像工学会, 日本生体医工学会, IEEE, SPIE 各会員.

江口 研二

1973 慶大・医卒. 1975 国立がんセンター中央病院内科医員. 1997 国立病院四国がんセンター副院長. 2002 東海大学医学部内科学系教授. 2008 帝京大学医学部内科学講座教授.

柿沼龍太郎

1978 福島県立医科大卒．1993 国立がんセンター東病院内視鏡部気管支内視鏡室医長．2004 国立がんセンターがん予防検診研究センター検診技術開発部画像診断開発室長．

森山　紀之

1973 千葉大・医卒．1976 国立がんセンター放射線診断部医員．1929 国立がんセンター東病院放射線部部長．1998 国立がんセンター中央病院放射線診断部部長．厚生労働省がん克服戦略研究事業総括及び主任研究者．国立がんセンターがん予防・検診研究センター長．

Radiol Phys Technol (2008) 1:244–250
DOI 10.1007/s12194-008-0036-z

Low-dose CT screening for lung cancer with automatic exposure control: phantom study

Shiho Gomi · Yoshihisa Muramatsu · Shinsuke Tsukagoshi · Masahiro Suzuki · Ryutaro Kakinuma · Ryosuke Tsuchiya · Noriyuki Moriyama

Received: 3 April 2008 / Revised: 11 June 2008 / Accepted: 11 June 2008 / Published online: 11 July 2008

Abstract We conducted a study to determine optimal scan conditions for automatic exposure control (AEC) in computed tomography (CT) of low-dose chest screening in order to provide consistent image quality without increasing the collective dose. Using a chest CT phantom, we set CT-AEC scan conditions with a dose-reduction wedge (DR-Wedge) to the same radiation dose as those for low-tube current, fixed-scan conditions. Image quality was evaluated with the use of the standard deviation of the CT number, contrast-noise ratios (CNR), and receiver-operating characteristic (ROC) analysis. At the same radiation dose, in the scan conditions using CT-AEC with the DR-Wedge, the SD of the CT number of each slice position was stable. The CNR values were higher at the lung apex and lung base under CT-AEC with the DR-Wedge than under standard scan conditions ($p < 0.0002$). In addition, ROC analysis of blind evaluation by four radiologists and three technologists showed that the image quality was improved for the lung apex ($p < 0.009$), tracheal bifurcation ($p < 0.038$), and lung base ($p < 0.022$) in the scan conditions using CT-AEC with the DR-Wedge. We achieved improvement of image quality without increasing the collective dose by using CT-AEC with the DR-Wedge under low-dose scan conditions.

Keywords Chest · Cancer screening · Low-dose · Computed tomography · Image quality · Automatic exposure control

S. Gomi (✉) · M. Suzuki · R. Kakinuma · N. Moriyama
Department of Cancer Screening Technology and Development, National Cancer Center Research Center for Cancer Prevention and Screening, 5-1-1 Tsukiji, Chuo-ku, Tokyo 104-0045, Japan
e-mail: sgomi@ncc.go.jp

Y. Muramatsu
Department of Diagnostic Radiology, National Hospital Organization Saitama National Hospital, 2-1 Suwa, Wakou-shi, Saitama 351-0102, Japan

S. Tsukagoshi
Department of CT Systems Division Application and Research Group, Toshiba Medical Systems Corporation, 1385 Shimoishigami, Otawara-Shi, Tochigi 324-8550, Japan

R. Tsuchiya
Department of Surgery, National Cancer Center Hospital, 5-1-1 Tsukiji, Chuo-ku, Tokyo 104-0045, Japan

1 Introduction

Because computed tomography (CT) scans provide a higher level of accuracy than that with chest radiography in detecting early lung cancer, chest CT screening is currently being performed as an additional means of secondary prevention to diminish lung cancer morbidity and its resultant mortality rate [1–5]. Chest CT screening should be performed at the lowest possible radiation exposure for healthy subjects. Therefore, currently chest CT screening is performed under the scan condition of a fixed low tube current [1–5]. However, the scan condition of a fixed low tube current has been a problem in that the image quality differs depending on the slice position and the individual subject [6, 7].

Itoh et al. [8, 9] showed that the minimum tube current required for helical CT in lung cancer screening differs depending on the location in the lung, and an ideal CT protocol for the lung requires a method for changing the tube current during helical scanning. Additionally, Li et al. [10] reported that, among the technologic innovations for

managing the radiation dose, CT automatic exposure control (CT-AEC) is the most important technique for maintaining a constant image quality while optimizing the radiation dose.

At present, multi-slice CT (MSCT) diffused scan systems include CT-AEC as an additional feature. Based on the initial scanogram, or scout view, CT-AEC adjusts the tube current with every rotation of the gantry, resulting in optimal image quality and a low patient dose. Therefore, a positioning scan is necessary when CT-AEC is used.

Although CT-AEC has been used in clinical practice [11–14] recently, it has almost never been used in chest CT screening. We believe that there are two primary reasons. First, under low tube current conditions, the effectiveness of CT-AEC is reduced due to limitations of the minimum tube current value and the interval setting. Second, a reduction in screening efficiency perhaps occurs because a scanogram must be performed for obtaining the water-equivalent thickness of target object data [15]. Furthermore, under scan conditions with the use of CT-AEC, there is the possibility that the collective dose could be higher than that under fixed low tube current scan conditions, depending on the image quality level setting and the maximum tube current setting. For these reasons, CT-AEC has not been used for chest CT screening, and a recommended optimal scan condition with CT-AEC has never been shown. However, it is important that optimal scan conditions of the CT-AEC are identified, because CT-AEC is required for chest CT screening [8, 9].

Our aim in the present study was to identify the optimal scan conditions by using CT-AEC so as to obtain a consistent image quality without increasing the collective dose under low-dose CT scan conditions.

2 Materials and methods

We used an Aquilion 16-slice CT scan system (Toshiba, Tokyo, Japan) equipped with the CT-AEC function. This CT scan system has three types of filters with a small wedge (S-Wedge), a large wedge (L-Wedge), and a dose-reduction wedge (DR Wedge). Figure 1 is a schematic representation of these filters. These filters were all made of aluminum. The S- and L-Wedges are commonly used for general examination, the DR-Wedge for CT fluoroscopy [16] and CT screening examination. The S-Wedge is used for a small body size of the examinee, the L-Wedge for a large size of the examinee. The S-Wedge was adapted to S (240 mm) and M (320 mm) sizes of the scan field of view (FOV). The L-Wedge was adapted to L (400 mm) and LL (500 mm) sizes of scan FOV. The DR-Wedge eliminated the soft rays for reduction of radiation exposure, and the aluminum thickness of the DR-Wedge was seven times greater than that of the L-Wedge. Therefore, the reduction of image contrast was apparent in the low-contrast region, but was effective for high-contrast regions, such as the chest. In addition, the DR-Wedge improves the image quality more than the conventional flat wedge does, and the radiation exposure was reduced by about 50%.

2.1 Scan conditions and phantom

Our institutional screening scan conditions were 120 kVp, 30 mA, 0.5 s/rotation, pitch factor (PF) 0.69, and 1 mm × 16 rows. We assumed that these scan conditions were the "standard scan conditions." Figure 2 shows the lung screening CT (LSCT) phantom (LSCT001, Kyoto Kagaku Company, Tokyo, Japan) [17, 18] used in this

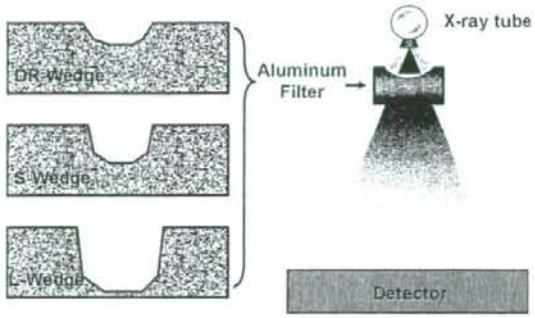

Fig. 1 Schematic representation of the filters. *Left*: from the top, dose reduction wedge (DR-Wedge), small wedge (S-Wedge), large wedge (L-Wedge). *Right*: schematic representation of CT. The DR-Wedge is an aluminum filter that is thicker than a general filter. The aluminum thickness of the DR-Wedge is seven times greater than that of the L-Wedge. This filter eliminates soft X-rays, and it can reduce the radiation exposure by 50%

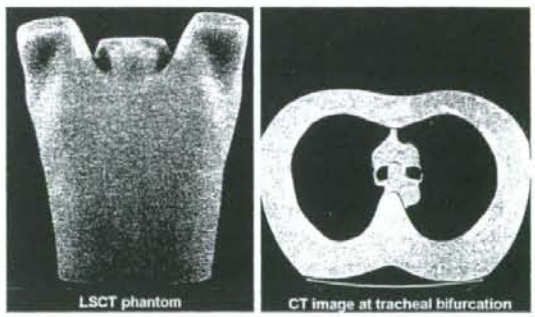

Fig. 2 Lung screening CT (LSCT) phantom. The LSCT phantom is a lung phantom of a Japanese man of standard physique (60 kg). Placement of simulated tumors (*spheres*) is bilateral in the lung apex, tracheal bifurcation, and lung base. Right lung: target contrast was 100 Hounsfield units (HU), and spheres were 4–12 mm in diameter (in 2-mm steps). Left lung: target contrast was 270 HU, and spheres were 2–10 mm in diameter (in 2-mm steps)

study. The LSCT phantom is a simulated lung of a Japanese man with a standard physique (60 kg). The target CT value of the simulated lung is −900 Hounsfield units (HU). The LSCT phantom had simulated tumors (spheres) in both lungs of each of five sizes that were located in the lung apex, tracheal bifurcation, and lung base. In the right lung, the target contrast was 100 HU, and the spheres were 4–12 mm in diameter (in 2-mm steps). In the left lung, the target contrast was 270 HU, and the spheres were 2–10 mm in diameter (in 2-mm steps).

In order to obtain target object data for the LSCT phantom, we determined CT-AEC scan conditions so that the dose length product value in air (DLP_{air}) was equal to or lower than the standard scan conditions. The phantom was placed at the center of rotation, and a scanogram was obtained to record target object data. The phantom was then removed, and a pencil-shaped ionization chamber dosimeter (Tomorad Systems, Capintec, PA) was placed at the rotation center for measurement of the DLP_{air} value under standard scan conditions (DLP_{air}-standard). The scan range was 350 mm. Based on this DLP_{air}-standard value, scan conditions with CT-AEC were determined both with and without the DR-Wedge. The scan conditions of CT-AEC were set manually so that the peak value of the tube current was located at the lung base. The phantom was placed once again at the center of rotation, and raw data on the phantom were acquired under the same scan conditions as indicated above. Image reconstruction was performed by use of raw data with a 5-mm reconstruction slice thickness, 1-mm reconstruction interval, and the image reconstruction kernel was FC01 for abdominal kernel with beam-hardening correction. For each scan condition, the tube current values were recorded every tube rotation during the LSCT phantom scanning with software developed in-house.

2.2 Image analysis and statistical analysis

Image quality was evaluated based on the standard deviation (SD) of the CT number, the contrast-noise ratio (CNR), and receiver-operating characteristic (ROC) analysis. The SD of the CT number was measured by software developed in-house at the square region of interest (ROI) set at the center of the reconstructed image. The ROI is shown in Fig. 3a. These measurement points precisely reflected the image noise in a homogeneous material. The CNR was calculated with the following equation:

$$\mathrm{CNR} = \sqrt{\frac{SD_W^2 - SD_B^2}{SD_B^2}}.$$

SD_W is the SD of the simulated tumor, and SD_B is the SD of the simulated lung. Figure 3b shows measurement points of SD_W (the simulated tumor in the left lung;

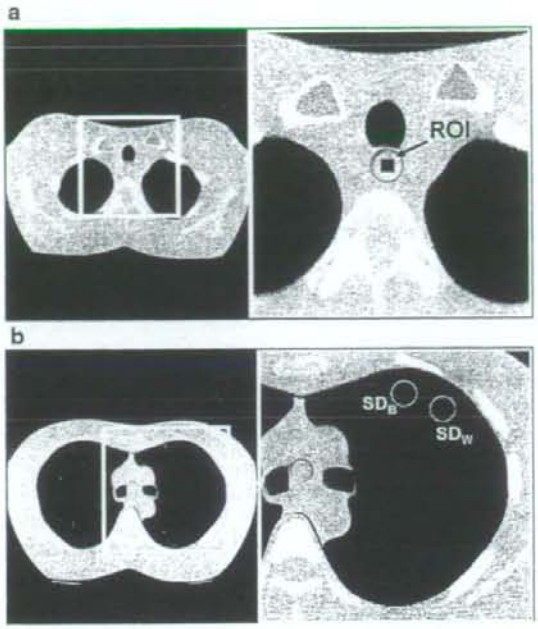

Fig. 3 **a** The standard deviation (SD) of the CT number was measured by software developed in-house at the square region of interest (ROI). These measurement points precisely reflected the image noise in a homogeneous material at center of the LSCT phantom. **b** Contrast noise ratio (CNR) measurement points on the simulated tumor in the left lung (10 mm, 270 HU). SD_W is the SD of the simulated tumor, and SD_B is the SD of the simulated lung

10 mm, 270 HU) and SD_B. ROC analysis [19] was performed for both standard scan conditions and CT-AEC with the DR-Wedge. The target objects were 60 images of simulated tumors in the right lung apex, tracheal bifurcation, and lung base and 60 images of simulated lung tissue around the simulated tumors. Figure 4 shows an example of a tracheal bifurcation. A computer program used ROCKIT (Charles E. Metz, University of Chicago, Chicago, IL) [20]. Four radiologists and three technologists were asked whether simulated tumors were present, and then they evaluated the images independently and on a blind basis by using a discrete rating scale of five points. The significance of differences in the area under the curve (AUC) values was evaluated by use of Student's paired t-test. In general, $p = 0.05$ was considered to indicate a statistically significant difference.

2.3 Image quality level setting for CT-AEC

In order to set conditions for routine scans and equivalent dose scans in the present study, we selected the tube current manually. However, the SD value was necessary to appropriately control the tube current when employing the

image quality setting of CT-AEC in the Toshiba CT scan system. We confirmed several SD values for image quality setting function so that tube current modulation equal to CT-AEC with DR-Wedge was obtained.

3 Results

3.1 Absorbed dose and modulation of tube current

The DLP_{air} values for each scan condition are shown in Table 1. The DLP_{air}-standard value under standard scan conditions was 97 mGy. The DLP_{air} values under the scan conditions of CT-AEC with or without the DR-Wedge were 91 mGy and 92 mGy. These DLP_{air} values are lower than those under the standard scan conditions. The values of the maximum tube current are shown in parentheses in the table, when each scan condition was set manually. Figure 5a shows the relationship between the tube current and the slice position under the standard scan conditions and CT-AEC with or without the DR-Wedge. The tube current modulation changed greatly when scanning was done with CT-AEC and the DR-Wedge.

3.2 Image analysis and statistical analysis

Figure 5b shows the SD of the CT number corresponding to Fig. 5a. The SD of the CT number for each slice position was stabilized in the following order: CT-AEC with the DR-Wedge > CT-AEC without the DR-Wedge > standard scan conditions. As a result of using CT-AEC with the DR-Wedge, the image quality was appropriate at each slice from the apex to the lung base. Table 2 shows the CNR

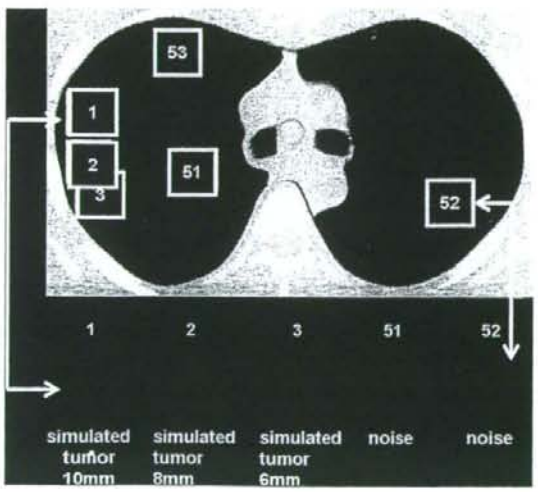

Fig. 4 Example of sample of receiver-operating characteristic (ROC) analysis at the tracheal bifurcation. The target objects were 60 images of simulated tumors in the right lung apex, tracheal bifurcation, and lung base and 60 images of simulated lung tissue around the simulated tumors

Table 1 Dose length product in air (DLPair) value and value of maximum tube current

	30 mA fixed	CT-AEC with dose reduction wedge	CT-AEC without dose reduction wedge
DLPair (maximum tube current)	96.96 mGy (30 mA)	90.71 mGy (120 mA)	92.46 mGy (40 mA)

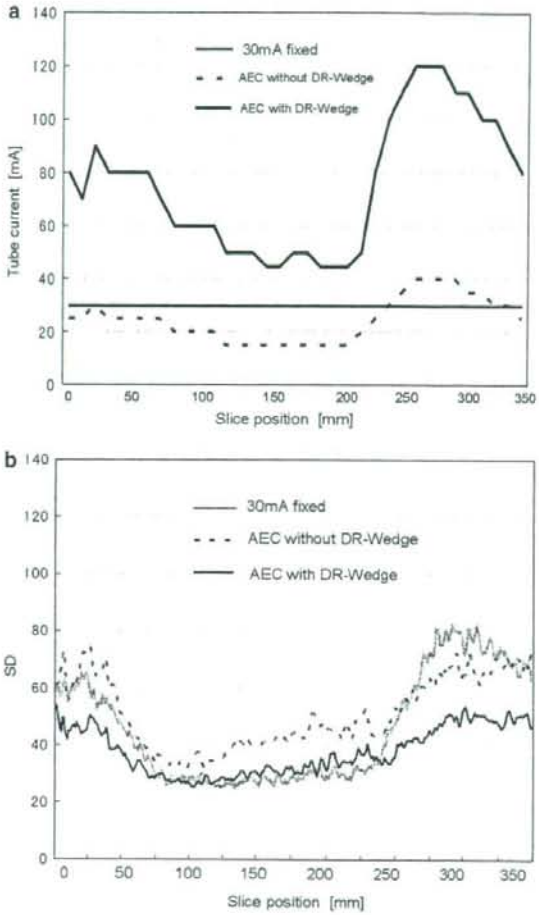

Fig. 5 a Relationship between the tube current and the slice position under the standard scan conditions and CT-automatic exposure control (CT-AEC) with or without the DR-Wedge. The tube current modulation changed greatly when scanning was done with CT-AEC and the DR-Wedge. b Standard deviation (SD) of the CT number corresponding to Fig. 5a

Table 2 Contrast noise ratio (CNR) values for each scan condition

	Lung apex	Tracheal bifurcation	Lung base
Standard scan conditions	1.67	2.58	2.83
CT-AEC without dose reduction wedge	1.6	2.18	2.67
CT-AEC with dose reduction wedge	1.9	2.5	3.2

values at the lung apex, tracheal bifurcation, and lung base under each set of scan conditions. The CNR values are higher at the lung apex and lung base under CT-AEC with the DR-Wedge than under standard scan conditions. A significant difference was found between the standard scan conditions and CT-AEC with the DR-Wedge ($p = 0.0002$). Figure 6 shows multiplanar reconstructions of the phantom images obtained under each of the scan conditions. Image quality was most homogeneous for CT-AEC with the DR-Wedge. Figure 7 shows the ROC curves for the lung apex, tracheal bifurcation, and lung base under standard scan conditions and for CT-AEC with the DR-Wedge. The AUC value of CT-AEC with the DR-Wedge was larger than the AUC of standard scan conditions in all of these regions, particularly in the lung apex. A significant difference was found between the two scan conditions at the lung apex ($p = 0.009$), tracheal bifurcation ($p = 0.038$), and lung base ($p = 0.022$).

3.3 Image quality level setting for CT-AEC

In our study, the CT-AEC scan conditions were set manually so that the tube current value peaked at the lung base. However, in examinations using CT-AEC with the Toshiba

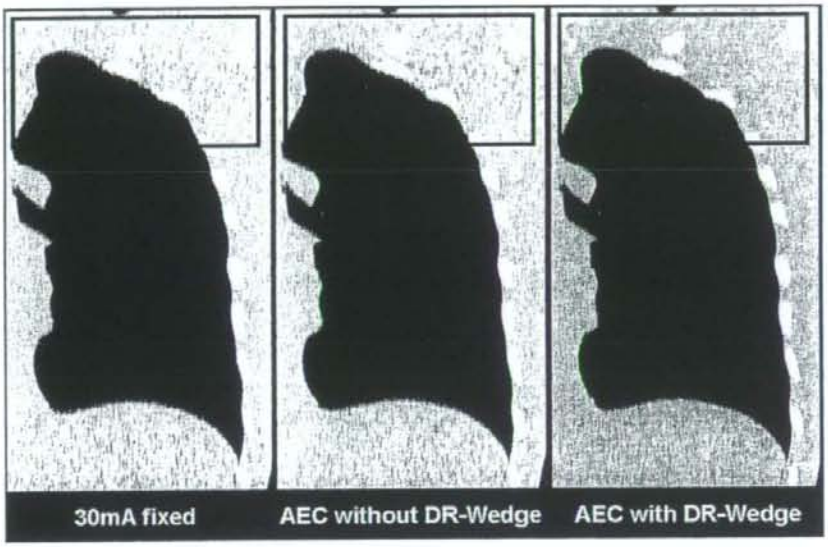

Fig. 6 Multiplanar reconstruction images of phantom obtained under standard scan conditions, CT-AEC without the DR-Wedge, and with the DR-Wedge. The image quality of CT-AEC with DR-Wedge was the most homogeneous

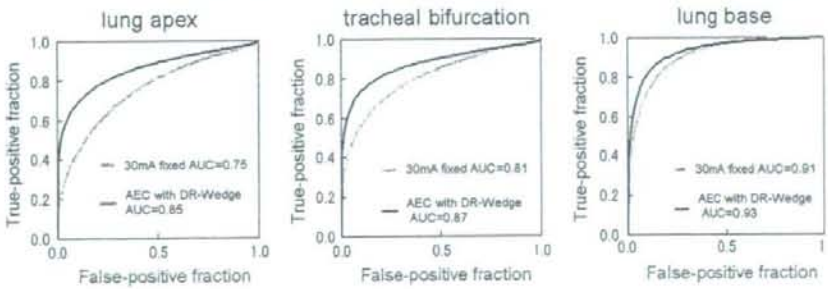

Fig. 7 ROC curves for standard scan conditions and CT-AEC with the DR-Wedge at the lung apex, tracheal bifurcation, and lung base. The area under the curve (AUC) of CT-AEC with the DR-Wedge was larger in all regions, particularly the lung apex. A significant difference was noted at the lung apex ($p = 0.009$), tracheal bifurcation ($p = 0.038$), and lung base ($p = 0.022$)

Aquilion CT scanner, a setting for the SD value is required. The results for manual settings were similar to the tube current settings when the image quality level was set at SD20 for CT-AEC, as shown in Fig. 8. CT-AEC with the DR-Wedge setting, therefore, with an image quality level of SD20 improved image quality and provided stable images as compared with standard scan conditions, without increasing the collective dose.

4 Discussion

For reducing the radiation dose, low-dose CT screening uses a fixed, lowest possible tube current. At the fixed lowest tube current, the image quality differed with the location of the lung, i.e., the apex, the base, and the other locations, and was based on the body size of the screenee. Therefore, to minimize the radiation dose, it is necessary to change the tube current when examining different locations in the lung with low-dose helical CT for lung cancer screening [8, 9]. As yet, however, there have been no studies of CT-AEC for chest CT screening. Therefore, we endeavored to use CT-AEC for low-dose chest CT screening. Our study had the following main results: A clear improvement in image quality was confirmed for CT-AEC with the DR-Wedge. There was no improvement in image quality when we used only CT-AEC at a low dose. This is because the tube current modulation changed only slightly when we used only CT-AEC scan conditions at a low dose. Therefore, CT-AEC with the DR-Wedge is useful for low-dose chest CT screening. In addition, we can expect a further radiation dose reduction for small screenees by using CT-AEC [21, 22]. It is important that we reduce the radiation dose, while maintaining the image quality necessary for a diagnosis.

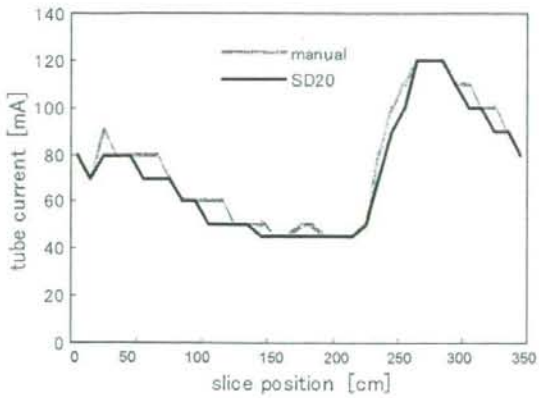

Fig. 8 Outputs at maximum tube current manual setting of 120 mA (lung base) and image quality level setting of SD20 for CT-AEC with the DR-Wedge

There are several limitations to our study. First, in this experiment, acquisition of a dosimeter covering a scan range (350 mm) of the LSCT phantom was difficult. Therefore, we set a dosimeter of 100 mm at the center of rotation of the CT device to measure this range and compared exposure doses for a scan range of 350 mm under each scan condition by measuring air exposure doses. Because we measured the exposure dose in the air, using the dosimeter measurement of exposure in the phantom will be necessary in the future. Second, with this CT-AEC system, a scanogram must be performed for obtaining target object data. If the minimum exposure conditions for the scanogram (80 kV, 10 mA, 5 s) are selected, the dose for the scanogram will be only about 2% of the DLP_{air}-standard value based on the results of preliminary experiments, but a reduction in throughput is unavoidable. Therefore, it would be ideal to perform CT-AEC without the need for a scanogram. In addition, because CT-AEC requires a similar lung-air volume for the scanogram and for actual scanning, it is particularly important to provide clear instructions concerning proper breathing to subjects who are to undergo screening examinations. Another limitation of our study is that the concept of setting of the SD value differs among manufacturers, and it cannot be used on scanners produced by other manufacturers.

In conclusion, based on standard scan conditions, optimization of chest CT screening conditions was studied on a 16-slice MSCT system equipped with a CT-AEC function. We achieved image quality improvement without increasing the collective dose by using CT-AEC with the DR-Wedge under low-dose scan conditions. The optimal scan conditions for screening examinations as determined by this study were 120 kV, 0.5 s/rotation, pitch factor 0.7, 1 mm × 16 rows, CT-AEC, a DR-Wedge, and SD20.

Acknowledgments We acknowledge the valuable assistance of the radiologists and the dedicated support for this project from all radiology personnel at the National Cancer Center Research Center for Cancer Prevention and Screening. The authors are grateful to Gen Iinuma, MD, Takashi Terauchi, MD, Nachiko Uchiyama, MD, Seiko Kuroki, MD, and Makoto Sugawara, MD, for participating as observers; to Kazuhisa Kainuma for image analysis; to Charles E. Metz, PhD, for the free software for ROC analysis that he offered; and to Miwa Okumura, Christopher Dix, Editor and Editorial Assistant of Radiological Physics and Technology for improving the manuscript. We are also grateful to Prof. J. Patrick Barron of the International Medical Communications Center of the Tokyo Medical University for his comments on the revised manuscript. This work was supported in part by a grant from the Third-Term Comprehensive 10-year Strategy for Cancer Control (H16-016, H16-020).

References

1. Kaneko M, Eguchi K, Ohmatsu H, Kakinuma R, Naruke T, Suemasu K, et al. Peripheral lung cancer, screening and detection with low-dose spiral CT versus radiography. Radiology. 1996;201:798–802.
2. Sone S, Takashima S, Li F, Yang Z, Honda T, Maruyama Y, et al. Mass screening for lung cancer with mobile spiral computed tomography scanner. Lancet. 1998;351:1242–5.
3. Henschke CI, McCaley DI, Yankelevitz DF, Naidich DP, McGuinness G, Miettinen OS, et al. Early lung cancer action project: overall design and findings from baseline screening. Lancet. 1999;354:99–105.
4. Henschke CI, Jae L, Wu N, Farooqi A, Khan A, Yankelevitz D, et al. CT screening for lung cancer: prevalence and incidence of mediastinal masses. Radiology. 2006;239:586–90.
5. Diederich S, Wormanns D, Heindel W. Low-dose CT: new tool for screening lung cancer? Eur Radiol. 2001;11:1916–24.
6. Yoshihara N, Matsumoto T, Fukuhisa K, Furukawa A, Yabe T, Nagano K, et al. Dose dependency of the image quality intended for lung cancer screening CT. J Thorac CT Screen. 2001;8:252–9. (in Japanese).
7. Muramatsu Y, Nakamura Y, Kubo M, Hanai K, Kimura H, Niki N. Lung cancer screening—balance of image quality and dose at low-dose chest CT. Jpn J Radiol Technol. 1999;55:1156–61. (in Japanese).
8. Itoh S, Ikeda M, Arahata S, Kodaira T, Isomura T, Yamakawa K, et al. Lung cancer screening: minimum tube current required for helical CT. Radiology. 2000;215:175–83.
9. Itoh S, Ikeda M, Mori Y, Suzuki K, Sawaki A, Iwano S, et al. Lung: Feasibility of a method for changing tube current during low-dose helical CT. Radiology. 2002;224:905–12.
10. Li J, Udayasankar UK, Toth TL, Seamans J, Small WC, Kalra MK, et al. Automatic patient centering for MDCT: effect on radiation dose. AJR Am J Roentgenol. 2007;188:547–52.
11. Kalra MK, Maher MM, D'souza RV, Rizzo S, Halpern EF, Blake MA, et al. Detection of urinary tract stones at low-radiation-dose CT with z-axis automatic tube current modulation: phantom and clinical studies. Radiology. 2005;235:523–9.
12. Flohr TG, Schaller S, Stierstorfer K, Bruder H, Ohnesorge BM, Schoepf UJ. Multi-detector row CT systems and image reconstruction techniques. Radiology. 2005;235:756–73.
13. Kalra MK, Maher MM, Toth TL, Hamberg LM, Blake MA, Shepard JA, et al. Strategies for CT radiation dose optimization. Radiology. 2004;230:619–28.
14. Kalra MK, Rizzo S, Maher MM, Halpern EF, Toth TL, Shepard JA, et al. Chest CT performed with z-axis modulation: scanning protocol and radiation dose. Radiology. 2005;237:303–8.
15. Toshiba Medical Systems USA Home Page, http://medical.Toshiba.com/clinical/radiology/aquilionmulti16-363-363-431,htm
16. Kato R, Katada K, Anno H, Suzuki S, Ida Y, Koga S. Radiation dosimetry at CT fluoroscopy: physician's hand dose and development of needle holders. Radiology. 1996;201:576–8.
17. Muramatsu Y. Quality control of chest CT screening by dedicated phantom. Jpn J Lung Cancer. 2005;43:1006–12. (in Japanese).
18. Muramatsu Y, Tsuda Y, Nakamura Y, Kubo M, Takayama T, Hanai K. The development and use of a chest phantom for optimizing scanning techniques on a variety of low-dose helical computed tomography devices. J Comput Assist Tomogr. 2003;27:364–74.
19. Shiraishi J, Utsunomiya A. Tests of statistically significant differences between two imaging systems in ROC analysis: use of the jackknife method and its application. Jpn J Radiol Technol. 1997;510:691–8. (in Japanese).
20. Metz's ROC software users group home page, http://www-radiology.uchicago.edu/krl/labrmcjp.htm.
21. Tack D, Meartelaer VD, Gevenois PA. Dose reduction in multidetector CT using attenuation-based online tube current modulation. AJR Am J Roentgenol. 2003;181:331–4.
22. Tsukagoshi S, Ota T, Okumura M, Muramatsu Y, Johkoh T. Simulator-assisted setting of scan protocols for X-ray CT: development and clinical usefulness of the Scan Plan Simulator. Jpn J Radiol Technol. 2006;62:95–104.

Ann Nucl Med (2008) 22:379–385
DOI 10.1007/s12149-008-0130-7

ORIGINAL ARTICLE

Evaluation of whole-body cancer screening using ^{18}F-2-deoxy-2-fluoro-D-glucose positron emission tomography: a preliminary report

Takashi Terauchi · Takeshi Murano · Hiromitsu Daisaki
Daisuke Kanou · Hiroko Shoda · Ryutaro Kakinuma
Chisato Hamashima · Noriyuki Moriyama
Tadao Kakizoe

Received: 4 September 2007 / Accepted: 8 January 2008

Abstract
Objective ^{18}F-2-deoxy-2-fluoro-d-glucose positron emission tomography (FDG-PET) is a promising screening modality targeting whole body. However, the validity of PET cancer screening remains to be assessed. Even the screening accuracy for whole-body screening using FDG-PET has not been evaluated. In this study, we investigated the screening accuracy of PET cancer screening.
Methods A total of 2911 asymptomatic participants (1629 men and 1282 women, mean age 59.79 years) underwent both FDG-PET and other thorough examinations for multiple organs (gastrofiberscopy, total colonofiberscopy or barium enema, low-dose thin section computed tomography and sputum cytology, abdominal ultrasonography, an assay of prostate-specific antigen, mammography, mammary ultrasonography, Pap smear for the uterine cervix, and magnetic resonance imaging for the endometrium and ovaries) between February 2004 and January 2005, and followed sufficiently. The detection rate, sensitivity, specificity, and positive predictive value of FDG-PET were calculated using cancer data obtained from all examinations along with a 1 year follow-up.
Results From among 2911 participants FDG-PET found 28 cancers, 129 cancers were PET negative. PET-positive cancers comprised seven colorectal cancers, four lung cancers, four thyroid cancers, three breast cancers, two gastric cancers, two prostate cancers, two small intestinal sarcomas (gastrointestinal stromal tumors), one malignant lymphoma, one head and neck malignancy (nasopharyngeal carcinoid tumor), one thymoma, and one hepatocellular carcinoma. PET-negative cancers included 22 gastric cancers and 20 prostate cancers that were essentially difficult to detect using FDG-PET. The overall detection rate, sensitivity, specificity, and positive predictive value were estimated to be 0.96%, 17.83%, 95.15%, and 11.20%, respectively.
Conclusions FDG-PET can detect a variety of cancers at an early stage as part of a whole-body screening modality. The detection rate of PET cancer screening was higher than that of other screening modalities, which had already shown evidence of efficacy. However, the sensitivity of PET cancer screening was lower than that of other thorough examinations performed at our institute. FDG-PET has some limitations, and cancer screening using only FDG-PET is likely to miss some cancers.

Keywords FDG-PET · Cancer screening · Screening value · Sensitivity · Evidence

T. Terauchi (✉) · T. Murano · H. Daisaki · D. Kanou · H. Shoda · R. Kakinuma
Screening Technology and Development Division, Research Center for Cancer Prevention and Screening, National Cancer Center, 5-1-1 Tsukiji, Chuo-ku, Tokyo 104-0045, Japan
e-mail: tterauch@ncc.go.jp

C. Hamashima
Screening Assessment and Management Division, Research Center for Cancer Prevention and Screening, National Cancer Center, Tokyo, Japan

N. Moriyama
Research Center for Cancer Prevention and Screening, National Cancer Center, Tokyo, Japan

T. Kakizoe
National Cancer Center, Tokyo, Japan

Introduction

In 2004, the Japanese government initiated the third-term comprehensive 10-year strategy for cancer control, aimed at reducing the incidence and mortality of cancer in Japan. The Research Center for Cancer Prevention and Screening (RCCPS) was established at the campus of the National Cancer Center, Tokyo, in the same year [1]. Although the development of new screening modalities is worthwhile, a systematic approach for evaluating cancer-screening programs is required. To investigate the efficacy of cancer screening, programs using new modalities, including ^{18}F-2-deoxy-2-fluoro-D-glucose positron emission tomography (FDG-PET), have been conducted.

FDG-PET is a technique that reflects the changes in glucose metabolism in tumor cells [2], and has been widely used clinically to differentiate between benign and malignant tumors [3], assess the effectiveness of chemotherapy or radiotherapy [4], and predict prognosis [5–7]. The potential of FDG-PET in the early detection of various cancers has received much attention because the test enables the whole body to be scanned simultaneously and non-invasively [8]. Because of this advantage, much enthusiasm for PET screening exists in Japan. About 60% of facilities in Japan that are equipped with PET machines offer PET examinations to individuals hoping to undergo cancer screening opportunistically.

However, the validity of FDG-PET for cancer screening remains unconfirmed, and the sensitivity of FDG-PET screening targeting the whole body has not been sufficiently measured. Therefore, in the present study, we investigated the sensitivity of FDG-PET for the detection of malignant tumors in asymptomatic individuals who underwent the RCCPS cancer-screening program.

Materials and methods

The RCCPS cancer-screening program is a one-arm prospective study designed to evaluate the efficacy of multiple cancer-screening modalities (Table 1) [1]. This is a hospital-based program, and participants are enrolled on a voluntary basis. The target group consisted of men aged 50 and above, and women aged 40 and above. The exclusion criteria were a previous diagnosis of cancer, or follow-up of pre-cancerous disease on the basis of self-reported medical histories. All participants signed informed consent documents that had been approved by the National Cancer Center.

The basic programs consisted of screenings for esophageal, gastric, colon, rectal, lung, hepatic, gallbladder, pancreatic, and renal cancers. The cancer-screening modalities that were examined were as follows: gastrofiberscopy (GFS) for the esophagus and stomach, total colonofiberscopy (TCF) or barium enema (BE) for the colon and rectum, low-dose thin section computed tomography (CT) and sputum cytology for the lung, and abdominal ultrasonography (US) for the liver, gallbladder, pancreas, and kidneys. The participants could choose to undergo a TCF or BE on the basis of their preferences. GFS and TCF were performed using a magnifying endoscope. For men, prostate cancer screening was performed using an assay of prostate-specific antigen (PSA) serum levels with a cut-off value of 2.7 ng/ml. For women, a combination of modalities was performed: a two-view mammography (MMG), US, and physical examination (PE) for the breasts, Pap smear for the cervix, and magnetic resonance imaging (MRI) for the endometrium and ovaries. Moreover, whole-body scanning using FDG-PET was provided as an optional investigation.

Table 1 Comprehensive screening program and target organs

Modality	Target organ
Gastrofiberscopy	Esophagus, stomach
Total colonofiberscopy or barium enema	Colon, rectum
CT* and sputum cytology	Lung
Abdominal US	Liver, GB, pancreas, kidneys
PSA	Prostate
MMG, mammary US, and PE	Breast
Cytology of uterine cervix	Uterine cervix
Pelvic MRI	Uterus, ovary
FDG-PET (and whole-body CT)	Whole body

US ultrasonography, *PSA* prostate-specific antigen, *PE* physical examination, *GB* gallbladder, *MMG* mammography, *MRI* magnetic resonance imaging, *FDG-PET* ^{18}F-2-deoxy-2-fluoro-D-glucose positron emission tomography, *CT* computed tomography
*Low-dose helical thin section CT

The FDG-PET images were obtained using two multiring PET scanners (ECAT Accel, Siemens, Knoxville, TN, USA and CTI, Knoxville, TN, USA) with a transaxial resolution of 6.2 mm at full-width half maximum. The individuals were required to fast for at least 5 h prior to the PET scan; 60 min after the injection of 2.78 MBq/kg of FDG (within a range of the manufacturer's recommended value) that had been produced in our radiopharmacy, emission and transmission scans were obtained from the head to the inguinal region. Three-dimensional emission scans were acquired for eight or nine bed positions at 2 min per position, followed by two-dimensional transmission scans at 1 min per position to correct for photon attenuation using a